


 Cite this: *RSC Adv.*, 2021, 11, 39657

# Fabrication and characterization of polyamide thin-film composite membrane *via* interfacial polycondensation for pervaporation separation of salt and arsenic from water

 Minh-Xuan Pham,<sup>ab</sup> Thu Minh Le,<sup>ab</sup> Thien Trong Tran,<sup>ab</sup> Huynh Ky Phuong Ha,<sup>ab</sup> Mai Thanh Phong,<sup>ab</sup> Van-Huy Nguyen<sup>bc</sup> and Le-Hai Tran<sup>ab</sup>

Pervaporation, mainly utilized to separate azeotropic mixtures, has been paid much attention for desalination in recent years due to its numerous advantages. The membranes based on thin-film composite structure have gained great interest in pervaporation due to their thin thickness, controllable hydrophilicity, and crosslinking density which affects the permeation flux and selectivity of the membranes. In this study, a polyamide thin-film composite (PA-TFC) membrane was fabricated through interfacial polymerization between amine monomers and trimesoyl chloride (TMC) on a polysulfone porous substrate (PSf). Four different diamine monomers, including ethylenediamine (EDA), triethylenetetramine (TETA), *m*-phenylenediamine (MPD), and piperazine (PIP) were used to investigate the effect of the monomers on the pervaporation performance of the resulting membrane for separation of sodium chloride (NaCl) and arsenate (As(v)) aqueous solution. The physicochemical properties of the membrane were characterized using attenuated total reflection Fourier transform infrared (ATR-FTIR), scanning electron microscopy (SEM), atomic force microscopy (AFM), and pure water contact angle measurement. Furthermore, the performance of the fabricated membranes was studied by pervaporation separation of 0.15 mg L<sup>-1</sup> As(v) and 5 g L<sup>-1</sup> NaCl aqueous solution at 40 °C, respectively. The results show that the rejections of the membrane are insignificantly affected by the chemical structures of the amines, and both the As(v) rejection and NaCl rejection are higher than 99.9%. However, the permeation flux decreases in the order of PIP-TMC membrane > TETA-TMC membrane ~ EDA-TMC membrane > MPD-TMC membrane. Furthermore, the operating conditions are found to affect the separation performance of the PIP-TMC membrane significantly. In particular, the elevating operation temperature profoundly increases the permeation flux, while the increase in high salt concentration leads to a slight decrease in rejection but a significant decline in permeation flux. The derived membrane shows a reasonable permeation flux of 16.1 kg m<sup>-2</sup> h<sup>-1</sup> and ca. 99.9% rejection for 1.5 mg L<sup>-1</sup> As(v) removal, as well as 13 kg m<sup>-2</sup> h<sup>-1</sup> and 99.3% rejection for 30 g L<sup>-1</sup> NaCl separation at 60 °C. The sufficient permeation flux and good rejection of As(v) and NaCl of the membrane suggested the promising application of PA-TFC membrane for pervaporation removal of toxic arsenic from water and desalination of seawater.

 Received 9th October 2021  
 Accepted 6th December 2021

DOI: 10.1039/d1ra07492j

[rsc.li/rsc-advances](http://rsc.li/rsc-advances)

## Introduction

The rapid growth of the global population, urbanization, and increasing water pollution have been considered to cause water security concerns worldwide. Apart from water preservation

techniques, such as preventing pollution discharge into rivers and lakes, seawater or brackish-water desalination and decontamination are the alternative solutions to produce available and pure drinking water.<sup>1,2</sup> Reverse osmosis (RO) membrane technology has been predominantly applied to desalination nowadays due to its advantages such as large production capacity and a simple operation process as compared with traditional distillation technology.<sup>1,3</sup> However, the intrinsically high operation pressure to overcome the osmotic pressure of the salt solution requires high energy consumption and results in membrane fouling, which limits the broad application of the RO technology.<sup>4</sup> The pervaporation membrane has emerged as

<sup>a</sup>Faculty of Chemical Engineering, Ho Chi Minh City University of Technology (HCMUT), 268 Ly Thuong Kiet Street, District 10, Ho Chi Minh City, Vietnam. E-mail: [mtphong@hcmut.edu.vn](mailto:mtphong@hcmut.edu.vn); [tranlehai@hcmut.edu.vn](mailto:tranlehai@hcmut.edu.vn)

<sup>b</sup>Viet Nam National University Ho Chi Minh City, Linh Trung Ward, Thu Duc District, Ho Chi Minh City, Vietnam

<sup>c</sup>Faculty of Biotechnology, Binh Duong University, Thu Dau Mot, Vietnam. E-mail: [mhuy@bdu.edu.vn](mailto:mhuy@bdu.edu.vn)



a promising alternative for desalination and removal of toxic ions in recent years because of its low energy requirement, high salt selectivity, and low fouling phenomena.<sup>5,6</sup> The transport mechanism of the process is based on the solution–diffusion theory; accordingly, the water molecules are preferentially adsorbed onto the feed side of a dense membrane and selectively diffused through the membrane to evaporate on the permeate side under a vacuum condition, while the salt or toxic ions are retained. The driving force of the pervaporation is the difference in the partial vapor pressure between the feed and the permeate sides of the membrane.<sup>4,7</sup>

In this process, the pervaporation membrane plays a crucial role in the separation performance. Therefore, the membrane should have high permeation flux, good selectivity, and excellent mechanical and thermal stability.<sup>6,7</sup> Many organic and inorganic materials are studied to fabricate pervaporation membranes, such as silicate, ZSM-5, NaA zeolite, cellulose acetate, polyester.<sup>4</sup> Among many polymer materials, polyvinyl alcohol has been intensively used to fabricate the membrane for the pervaporation process because it exhibits good mechanical resistance and is cost-effective.<sup>8</sup> Nevertheless, the permeation flux of the membrane formed by the casting method is relatively low, and the membrane is susceptible to be swollen in the aqueous solution at high operation temperature, which affects the selectivity of the membrane.<sup>4,6–8</sup> Therefore, the membrane should be converted from a dense, thick layer into the asymmetrical or thin-film composite (TFC) structure to improve the permeation flux without an undesirable decline of selectivity.<sup>6,7</sup> Polyamide (PA), a hydrophilic material, is used to fabricate PA-based TFC membrane *via* interfacial polymerization (IP) between multifunctional amines and acyl chlorides on the top of micro-porous substrates.<sup>9</sup> The advantage of this approach is easy to form a thin (10–1000 nm) and dense selective PA layer. Moreover, the physicochemical properties of the membrane could be tailored by varying the synthesis conditions, such as the chemical structures of monomers, monomer concentration, fabrication procedures, solvents, and the properties of a support substrate.<sup>10</sup> Recently, PA-TFC membranes have been intensively developed for pervaporation separation of liquid mixtures, such as ethanol (EtOH)/water and isopropanol (IPA)/water.<sup>10–16</sup> The effect of chemical structures of amines on the properties and dehydration efficiency of 90 wt% IPA solution at 25 °C was investigated.<sup>12</sup> A relationship between the separation performance and the physicochemical properties was reported, including free volume space, surface roughness, and hydrophilicity of the PA selective layers. Li *et al.* successfully developed a PA-TFC membrane *via* IP of triethylenetetramine (TETA) and trimesoyl chloride (TMC) on the top of modified polyacrylonitrile (PAN) support for pervaporation separation of IPA solution. The report demonstrated that the synthesis conditions, such as monomer concentrations and reaction time, significantly affect the morphology and separation efficiency of the membrane.<sup>14</sup> Huang *et al.* systematically studied the influences of chemical structures of amines on the separation performance of PA-TFC membrane for dehydrating tetrahydrofuran (THF). It was reported that the free volume of the PA layer depends on the chemical structures of monomers, in which the

PA layers prepared by linear aliphatic amines show a smaller free volume than cyclic and aromatic amines.<sup>17</sup> Furthermore, Tsai *et al.* demonstrated that the increase in the number of functional amines on the chain of amines can improve the selectivity of the PA-TFC membrane for pervaporation dehydration of EtOH solution through increasing crosslinking degree in PA layers.<sup>16</sup>

To our best knowledge, there are few studies on the preparation of PA-TFC membrane for pervaporation desalination and removal of toxic ions from water. The researchers have focused on fabricating graphene-based membrane and GO-based nanocomposite membranes for desalination.<sup>18–21</sup> Huang *et al.* reported a novel GO-polyimide hollow fiber membrane with a water flux of 15.6 kg m<sup>-2</sup> h<sup>-1</sup> and a salt rejection of 99.8% for desalination of 3.5 wt% seawater.<sup>20</sup> Zhao *et al.* studied fabricating a polyamide-graphene oxide (PA-GO) composite membrane by vacuum filtration combined with IP to upgrade the pervaporation desalination performance of hypersaline solutions.<sup>21</sup> It shows that PA plays a role in stabilizing the GO layer, and the GO thickness controls the water flux and selectivity of the membrane. The fabricated membrane exhibited a high water flux of 24–26.7 kg m<sup>-2</sup> h<sup>-1</sup> and excellent rejection of 99.99% for the desalination of NaCl aqueous solutions (3.5–10 wt%).

In the present work, PA-TFC membranes are fabricated for pervaporation separation of the arsenic contamination (such as As(v) of arsenic salt (Na<sub>2</sub>AsHSO<sub>4</sub>·7H<sub>2</sub>O)) in aqueous salt solutions. In particular, several amine monomers with different chemical structures and functional amine groups, such as ethylenediamine (EDA), triethylenetetramine (TETA), piperazine (PIP), and meta-phenylenediamine (MPD), are used to react to trimesoyl chloride (TMC) *via* IP process on the surface of the polysulfone porous substrate. The influence of chemical structures of the amines and the operation conditions on the pervaporation performance of the prepared membranes are also investigated. This study is expected to shed light on developing a TFC membrane with improved permeation flux and selectivity for simultaneous pervaporation removal of toxic arsenic from water and desalination of seawater.

## Experimental

### Materials

Reagents for the synthesis of polyamide membrane, including ethylenediamine (purity 98%) (EDA), triethylenetetramine (purity 97%) (TETA), *m*-phenylenediamine (MPD), and trimesoyl chloride (TMC) with a purity of 99%, were purchased from Sigma-Aldrich (USA). *n*-Hexane (99%) provided by Merck, and deionized water (conductivity ≤ 4 μS cm<sup>-1</sup>) were used as solvents for the IP synthesis. Polysulfone porous membrane (PS20) received from Sepro membranes (USA) was used as the mechanical substrate for fabricating PA-based thin-film composite membrane (PA-TFC) for pervaporation separation of salt and arsenic from water. Sodium chloride (NaCl) and arsenic salt (Na<sub>2</sub>AsHSO<sub>4</sub>·7H<sub>2</sub>O) purchased from Guangzhou Zio Chemical (China) were used for making synthesized salt solutions.

### Preparation of thin-film composite membrane

The polyamide thin film was hand-cast on the PS20 substrate through an IP process.<sup>3,9</sup> The PA-TFC membrane was formed by immersing the wetted support membrane in a 2.5 wt% diamine aqueous solution for 5 min. After that, the excess diamine solution was removed from the support membrane surface using an air knife (Exair Corporation) at about 4–6 psi. The diamine saturated support membrane was then immersed into a 0.5 wt% TMC-hexane solution for 3 min. The reacting surface was rinsed with hexane to remove the unreacted solution before drying in air at an ambient temperature for 1 min. Then, the prepared membrane was heated in an oven at 60 °C for 20 min. The resulting membrane was washed in water overnight and finally stored in deionized water before its use.

### Membrane characterization

The surface chemistry of the PA-TFC membrane was characterized using a Fourier transform infrared (FTIR) spectrometer (IFS28, Bruker) with an attenuated total reflection (ATR) supplied by the PIKE MIRacle™ (USA). A total of 60 scans were made for each sample with an apparatus resolution of 10 cm<sup>-1</sup>. The water contact angle (CA) of the membrane surface was measured using a contact angle analyzer (OCA25, Dataphysics). Five measurements were made at different locations at room temperature for each membrane sample, and the average value was reported. The surface morphology of the membrane, especially surface roughness, was characterized by the atomic force microscope (XE7-AFM, Park Systems). The top surface and cross-section morphologies of the membrane were visualized using the field emission scanning electron microscope (S-4800 FESEM, Hitachi).

### Pervaporation experiments

The separation performance of prepared membranes was tested with aqueous NaCl (5000 ppm) and As(v) (150 ppb) solutions, using a lab-scale pervaporation unit with an effective membrane area of 21 cm<sup>2</sup>. The schematic diagram of the pervaporation setup is illustrated in Fig. 1.

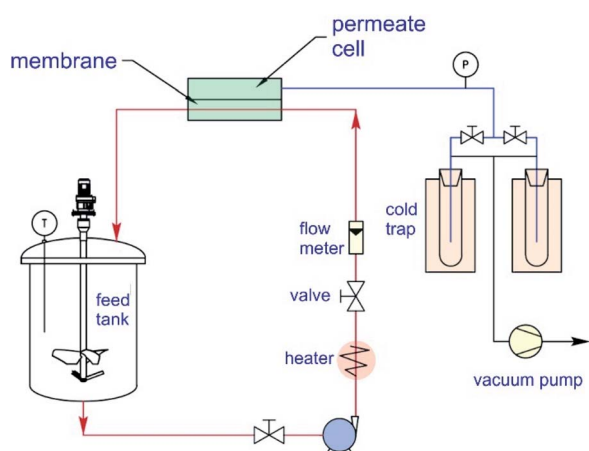


Fig. 1 The schematic illustration of a lab-scale pervaporation unit.

The feed solution was circulated from the feed tank through the membrane cell with a flow rate of 90 L h<sup>-1</sup> by a feed pump (Catpumps, USA). The feed solution temperature was maintained at 40 ± 1 °C by a laboratory recirculating heater. The pressure of the feed side was at atmospheric pressure, and the pressure on the permeate side was maintained at 3 mbar by using a vacuum pump (Robinair, USA). The separation process was conducted for 2 h, and the permeate vapor was condensed in a nitrogen liquid in a laboratory cold trap. The collected permeate was weighed using a mass balance (accuracy ± 0.0001 g) for determining the permeation flux at 25 °C. The permeation flux ( $J$ ) and the rejection of salt, as well as arsenic, were determined using eqn (1) and (2), respectively.

$$j(\text{kg m}^{-2} \text{h}^{-1}) = \frac{Q}{A \times t} \quad (1)$$

$$R(\%) = 1 - \frac{C_p}{C_f} \times 100\% \quad (2)$$

where,  $Q$  (kg) represents the weight of permeate collected within an operation time  $t$  (h), and  $A$  (m<sup>2</sup>) is the effective membrane area,  $C_p$  and  $C_f$  are the salt concentration of the feed and permeate solutions measured by a conductivity meter (HC9021-Pro, WalkLAB), respectively. For Arsenate solutions, the  $C_p$  and  $C_f$  are Arsenic concentrations of the feed and permeate solutions determined *via* an ICP analysis (ICP-EOS, Horiba), respectively. After each experiment, the pervaporation unit was rinsed two times with deionized water for 2 L to ensure the conductivity of a final rising solution was lower than 10 μS cm<sup>-1</sup>.

## Results and discussion

### Membrane characterizations

The chemical structures of the PA-TFC membranes prepared by different diamine monomers are characterized by FTIR, as shown in Fig. 2a. Compared with the spectrum of PSf substrate, the new peaks at 1541 cm<sup>-1</sup>, 1650 cm<sup>-1</sup>, and 1725 cm<sup>-1</sup> are correspondent to the vibration of N–H (amide II), C=O (amide I), and COOH groups, respectively.<sup>22–25</sup> The carboxylic acid groups arise from the hydrolysis of the acyl chlorides, which are unreacted with amine monomers.<sup>3</sup> As shown from Fig. 2b, the EDA-TMC and TETA-TMC membranes show prominent peaks at 1650 cm<sup>-1</sup>, while there is an unclear observation of peaks at 1725 cm<sup>-1</sup>, which implied a higher crosslinking degree of the membrane produced from aliphatic diamine monomers. In addition, there are two characteristic peaks at 1541 cm<sup>-1</sup> and 1725 cm<sup>-1</sup> for the PIP-TMC membrane, while the aromatic MPD-TMC shows typical peaks of the amide I, along with the shoulder peak 1725 cm<sup>-1</sup> characterized for the COOH groups. This suggests that the cyclic and aromatic diamine monomers could form the PA layers with a lower crosslinking degree and more carboxylic groups on their membrane surface. The FTIR spectra in Fig. 2 indicate the successful formation of a PA thin film on the polysulfone support membrane *via* the IP process.

The surface and cross-section morphologies of the PA-TFC membranes are investigated by FESEM measurement, and the

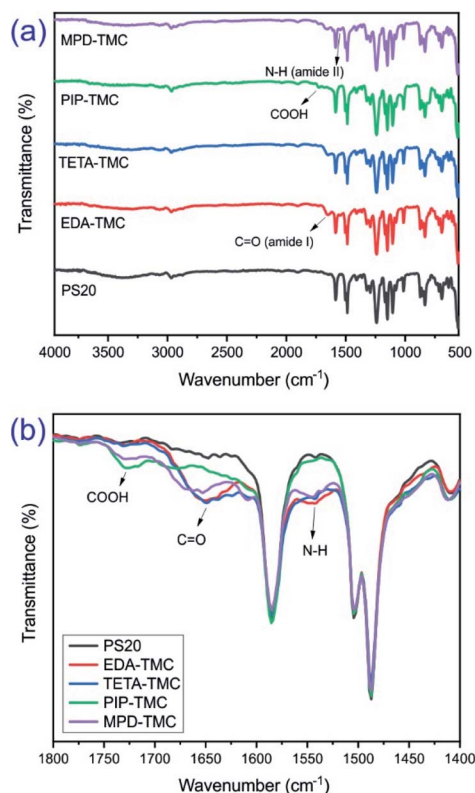


Fig. 2 ATR-FTIR spectra of the PS20 support and the four PA-TFC membranes in the regions: (a) 4000–500 and (b) 1800–1400  $\text{cm}^{-1}$ .

images are shown in Fig. 3. The visual observation reveals that the variation in the chemical structure of the amine monomers leads to differences in the morphology of the prepared membranes. Fig. 3a–d presents the surface morphologies of the prepared membranes. The three membrane surfaces, including EDA-TMC, TETA-TMC, and PIP-TMC, showed a nodular-like structure. As can be seen from Fig. 3a and b, the well-dispersed and tight-packed nodules are observed on the surfaces of EDA-TMC and TETA-TMC membranes. The difference in the nodular surface between EDA-TMC and TETA-TMC membrane is that nodules on the former are more extensive than that on the latter. Moreover, finely dispersed nodules could be observed with visible open pores distributing on the surface of the PIP-TMC membrane (Fig. 3c). This surface morphology is similarly reported in previous studies on the synthesis of poly(piperazine amide) membrane.<sup>24,26</sup> Meanwhile, the MPD-TMC membrane shows a ridge and valley morphology, together with a dense surface. As regards the cross-section of the synthesized membranes (Fig. 3e–h), the thickness of the membrane is found to decrease in the order of PIP-TMC > MPD-TMC > TETA-TMC > EDA-TMC. This phenomenon could be attributed to the chemical structure of amine monomers. It is generally known that the diffusion of amine monomers predominantly controls the physicochemical properties of the PA layer produced *via* IP to the interface between two immiscible solvents to react with TMC, and the reaction takes place in the organic side due to the low solubility of TMC in water.<sup>12,16,17</sup>

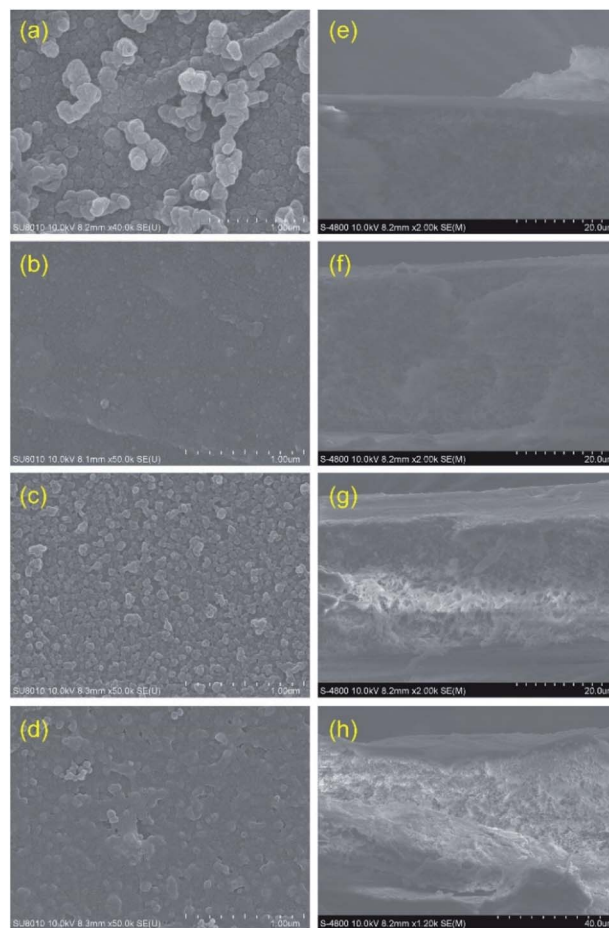


Fig. 3 Surface and cross-sectional SEM images of the four PA-TFC membranes: (a and e) EDA-TMC/PSf; (b and f) TETA-TMC/PSf; (c and g) PIP-TMC/PSf; (d and h) MPD-TMC/PSf.

Both EDA and TETA possess a linear aliphatic structure, but EDA has fewer alkyl units. Thereby, the diffusion rate to the reaction zone of EDA is higher than that of TETA, and thus it results in a denser and thinner PA layer, together with enhancing nodules on the membrane surface.<sup>14,16</sup> Compared with the linear aliphatic monomers, PIP and MPD own the alicyclic and aromatic conformations, respectively, resulting in the slower diffusion rate to the interfacial region for forming a loose PA thin-film. Thus, PIP and MPD could penetrate through the initially loose PA thin-film to further react with TMC to produce a thicker membrane. MPD is more rigidity and steric hindrance due to the aromatic ring-containing on its compound, leading to a production of the thinner membrane compared to the PIP monomer.<sup>10–12</sup>

Fig. 4 shows the AFM images of the prepared membranes and the surface roughness, in terms of average roughness ( $R_a$ ), root-mean-square roughness ( $R_{ms}$ ), and maximum roughness ( $R_{max}$ ) are respectively presented in Table 1. The results reveal that the surface roughness of the membrane increases in the order of PIP-TMC < EDA-TMC < MPD-TMC < TETA-TMC. TETA possesses a longer molecular chain and a more significant number of amine functional groups than EDA for the linear

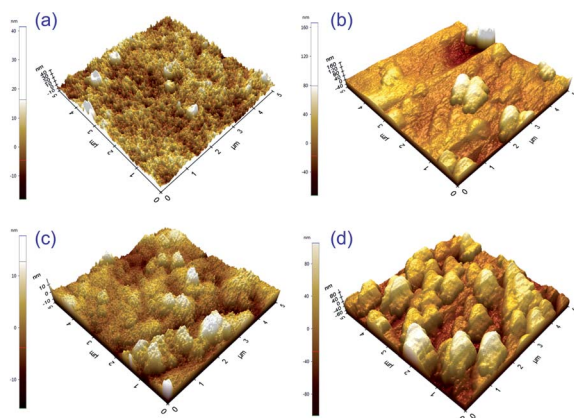


Fig. 4 AFM images of the four PA-TFC membranes: (a) EDA-TMC/PSf, (b) TETA-TMC/PSf, (c) PIP-TMC/PSf, (d) MPD-TMC/PSf.

Table 1 The surface roughness of the PA membranes prepared by different amine monomers

Membrane	$R_a$ (nm)	$R_{rms}$ (nm)	$R_{max}$ (nm)
EDA-TMC	3.49	4.08	16.74
TETA-TMC	15.53	19.57	64.74
PIP-TMC	0.98	1.22	4.93
MPD-TMC	10.24	12.24	49.22

aliphatic amine monomers. Thus, the relative surface of the TETA-TMC membrane is rougher than that of the EDA-TMC one.<sup>12,14</sup> As for the cyclic amine monomers, MPD has an aromatic ring, while PIP owns a heterocyclic ring. Therefore, the surface roughness of the MPD-TMC membrane is greater than that of the PIP-TMC membrane due to the higher steric hindrance of benzene rings contained in the MPD-TMC membrane.<sup>26,27</sup> Interestingly, PIP, a cyclic diamine compound with a larger molecular size and higher steric hindrance than the aliphatic EDA monomers, is expected to form a rougher PA thin film due to its relatively slow diffusion and lower reaction rate in comparison with EDA. However, the PA layer prepared by the PIP monomer shows a less rough surface compared with that formed by the EDA monomer. It could be due to the small nodular morphology and loose structure of the surface of the PIP-TMC membrane.<sup>10,12</sup>

In general, mass transport within the pervaporation membrane follows the solution-diffusion mechanism.<sup>4,7</sup> Therefore, the sorption capability of the membrane surface to the water molecules plays a vital role in the separation performance of the pervaporation membrane. The water contact angle could be employed to evaluate the sorption capability of the resulting membrane. The lower water contact angle demonstrates the higher hydrophilicity of the membrane. Fig. 5 illustrates the pure water contact angle of the PS20 support and the PA-TFC membranes synthesized by different amine monomers.

The results show that the hydrophilic property of the four PA-TFC membranes was higher than that of the PS20 substrate ( $73.5 \pm 2.2^\circ$ ), indicating that a hydrophilic PA layer was

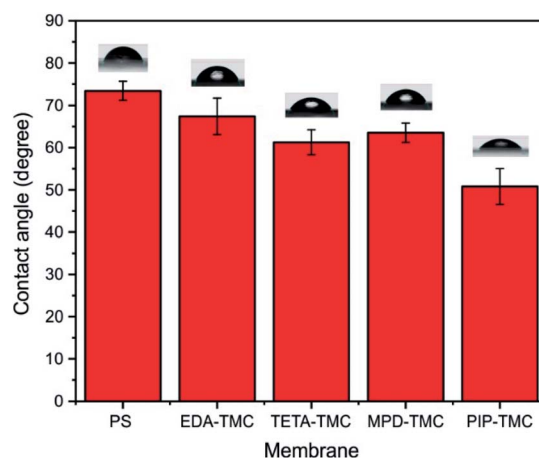


Fig. 5 The water contact angle of the PS20 support and the four PA-TFC membranes.

successfully synthesized on the support membrane. Among the PA-TFC membranes, the PA thin-film prepared by the EDA monomer shows the highest hydrophobic property, which could be attributed to the high diffusion and reaction rate of the EDA, resulting in the protruding globular morphology generated on the membrane surface.<sup>16</sup> The result is also agreed with the FTIR spectrum, showing a tremendous crosslinking extent of the EDA-TMC membrane (Fig. 2). Although there is a structural disparity between TETA and MPD, the hydrophilic properties of the PA thin films synthesized by the two monomers are pretty comparable. This result could be due to many functional groups, such as carboxylic acids or abundant amine resulting from the hydrolysis of the acyl chloride or the protonation of unreacted amines during the IP created on surfaces of the relative membranes.<sup>3</sup> Moreover, the high surface roughness could additionally contribute to the low hydrophilicity of the TETA-TMC membrane (Fig. 4b and Table 1). Remarkably, The PIP-TMC membrane surface exhibits the lowest hydrophilicity, arising from the low reaction rate of PIP with TMC to produce a loose membrane structure with an abundance of carboxylic functional groups.<sup>26</sup> It is worth noting that the combination of great hydrophilicity and high roughness could positively affect the separation performance of the derived membrane.

### Pervaporation performance

The separation performance of the PA-TFC membranes in terms of permeation flux and rejection are investigated through the separation of  $0.15 \text{ mg L}^{-1}$  As(v) and  $5 \text{ g L}^{-1}$  NaCl solutions at  $40^\circ\text{C}$ , respectively. The results are illustrated in Fig. 6.

It can be seen that a difference of the permeation flux with the order of  $\text{MPD-TMC} < \text{EDA-TMC} \sim \text{TETA-TMC} < \text{PIP-TMC}$  demonstrates the effect of the different chemical structures of the amine monomers on the permeation flux of prepared membranes. Moreover, the variation in permeation flux for separation of As(v) and NaCl solutions is relatively similar. Remarkably, the permeation flux for separating NaCl solution (Fig. 6b) is slightly lower than that for As(v) solution (Fig. 6a),

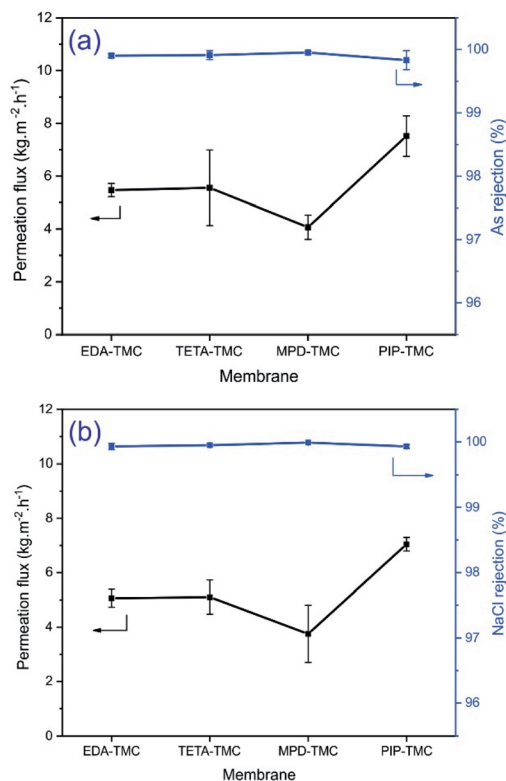


Fig. 6 Effect of the amine monomers on the separation of the four PA-TFC membranes for (a) As(v) removal and (b) NaCl separation.

which could be ascribed to the high NaCl concentration in the feed solution, resulting in a reduction of partial vapor pressure at high temperature (40 °C), which affects the permeation flux of the membrane.<sup>20,28</sup> However, the TETA-TMC membrane has higher surface roughness and more excellent hydrophilicity than the EDA-TMC membrane, which is favorable for improving permeation flux. The EDA-TMC and TETA-TMC membranes exhibit a comparable flux, which could be due to a large number of amine functional groups on the TETA, making an intensive crosslinking degree of the TETA-TMC layer.<sup>15,16</sup> This hinders the mobility of the polymer chain in the PA network even at a high operating temperature and hence prevents the diffusion of water molecules through the selective PA layer.<sup>14</sup> Compared with the linear aliphatic amine monomers, the MPD monomer produces a PA layer with a higher thickness and lower hydrophilic property, which is disadvantageous to the permeation flux of the membrane. Despite having a higher thickness, the PIP-TMC membrane shows a higher permeation flux, nearly twice the permeation flux of the MPD-TMC membrane. This phenomenon could be due to the more excellent hydrophilicity and a lower crosslinking degree in the PIP-TMC network.<sup>26</sup>

Apart from the permeation flux, rejection is also an essential parameter for evaluating the performance of the membrane. According to Fig. 6, all the PA membranes synthesized in this study exhibit an excellent rejection (>99.9%) of As(v) and NaCl. This observation is because the PA selective layer is regarded as one of the hydrophilic membranes, and the NaCl and As(v) solutions comprise volatile water species and bulkier hydrated

salt ions, which are non-volatile. Thereby, free water molecules are preferred to adsorb into the PA layer and selectively diffuse through the membrane based on the free volumes created by the thermal motion of polymer chains in the PA matrix, while salts are rejected.<sup>4</sup> Due to the comparable salt rejection of the derived membranes, it is suggested that PIP is a suitable functional diamine monomer to synthesize the PA-TFC membrane with high permeation flux, good As(v), and NaCl rejections.

### Operating condition effects

The pervaporation performance of the PA-TFC membrane prepared by PIP and TMC monomers *via* IP is evaluated with different operation conditions, including operating temperature, As(v) concentration, and NaCl concentration in the feed solution. Fig. 7 presents the permeation flux and As(v) rejection of the prepared membrane as a function of feed temperature for different As(v) concentrations in the feed solution.

The results show that the As(v) rejection is over 99.9% for all the experiments, indicating a negligible impact of operating temperature and As(v) concentration (0.15–1.5 mg L<sup>-1</sup>) on the As(v) rejection of the prepared membrane. On the contrary, the permeation flux increases significantly from 7.5 kg m<sup>-2</sup> h<sup>-1</sup> to about 22.8 kg m<sup>-2</sup> h<sup>-1</sup>, as elevating the operating temperature from 40 °C to 70 °C, while the effect of As(v) concentration in the feed solution is unremarkable. Compared with separating As(v) solutions, the permeation flux is found to be improved by increasing the feed temperature for the separation of NaCl solutions (Fig. 8). According to Raoult's law, the water vapor pressure could be raised 4 times when increasing the feed solution from 40 °C to 70 °C, leading to the approximately 3-fold permeation flux. This result is well consistent with previous findings.<sup>21,29,30</sup>

However, the variation of permeation flux is depended on the salt concentration in the feed solution. The increasing rate in the permeation flux for separating lower NaCl concentrations is more significant than that for rejecting higher ones. The phenomenon could be explained by the transport mechanism in the pervaporation membrane.<sup>6</sup> Raising operation

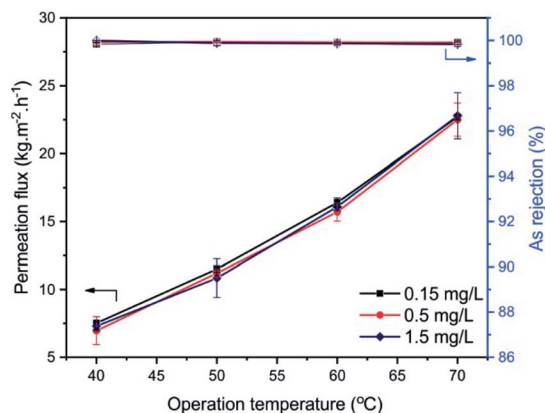


Fig. 7 Effect of operation temperature and As(v) concentration in the feed solution on the separation performance of the PIP-TMC membranes.

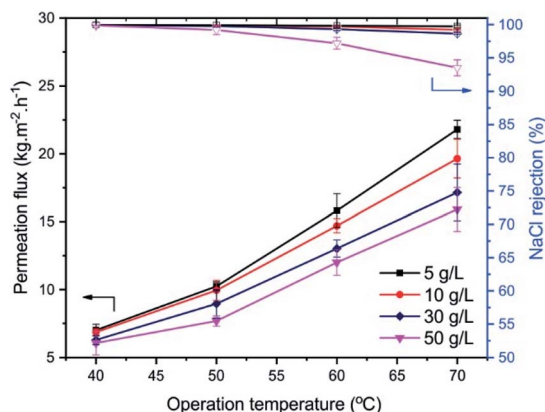


Fig. 8 Effect of operation temperature and NaCl concentration in the feed solution on the separation performance of the PIP-TMC membranes.

temperature could increase the water vapor pressure on the feed side of the membrane when the vapor pressure on the permeate side is maintained. As a result, it could enhance the driving force across the membrane, which increases the permeation flux of the membrane. Moreover, the different operation temperatures could increase the thermal motion of polymer chains, which extends the fractional free volume space in the PA matrix for improving the diffusion of free water molecules through the PA layer.<sup>20,21</sup>

The ion concentration in the feed side also exerts a detrimental effect on the permeation flux of the membrane.<sup>4</sup> The growth of ion concentration in the feed solution leads to a decrease in the water vapor pressure and the reduction of the free water molecules and, therefore, decreasing the permeation flux.<sup>4,6,7</sup> The results show that the low concentration of As(v) in the aqueous solution in the range of 0.15–1.5 mg L<sup>-1</sup> insignificantly influences the permeation flux of the membrane due to the slight difference in the water vapor pressure of the feed solution (Fig. 7). As opposed to the low As(v) concentration, the higher feed NaCl concentrations (5–30 g L<sup>-1</sup>) reduce the water vapor pressure, which leads to the relative decrease in the permeation flux (Fig. 8). It could be found that the permeation flux decreased by approximately 21% for pervaporation separation of 30 g L<sup>-1</sup> feed NaCl solution at 70 °C, in comparison with the separation of 5 g L<sup>-1</sup> NaCl solution at the same operating condition. The incremental operating temperature at high salt concentration could expand the free volume spaces in the PA selective layer *via* increasing the thermal motion of polymer chains and simultaneously increasing the diffusion rate of salt ions through the membrane.<sup>17,28</sup> This results in the decline of the salt rejection of the membrane. In this study, the NaCl rejection is observed to slightly decrease from over 99.9% to 98.7% with the extent of operating temperature and NaCl concentration of the feed solution (Fig. 8). Although the conditions for conducting experiments are different, it is worth comparing the separation performance in terms of permeation flux and NaCl, toxic rejections in the literature. The results in this study reveal that the membrane shows the permeation flux

of 16.1 kg m<sup>-2</sup> h<sup>-1</sup> and *ca.* 99.9% rejection for 1.5 mg L<sup>-1</sup> As(v) removal, as well as 13 kg m<sup>-2</sup> h<sup>-1</sup> and 99.3% rejection for 30 g L<sup>-1</sup> NaCl separation at 60 °C. At a higher temperature of 70 °C, the permeation flux is 22.8 kg m<sup>-2</sup> h<sup>-1</sup>, and the rejection is *ca.* 99.9% for As(v) removal, while the permeation flux is 17.2 kg m<sup>-2</sup> h<sup>-1</sup> and the lower rejection is 98.7% for separating NaCl solution. Compared with the pervaporation desalination membranes of PA-GO,<sup>21</sup> diamines modified graphene oxide nanosheets (Ax-GO),<sup>31</sup> polyvinyl alcohol (PVA),<sup>32,33</sup> MXene,<sup>34</sup> zeolites,<sup>35,36</sup> and polysulfonamide,<sup>37</sup> the PIP-TMC membrane exhibits a reasonable pervaporation performance with adequate permeation flux and good rejection.

## Conclusion

In the present work, the polyamide-based thin-film composite membrane is successfully synthesized on the polysulfone substrate *via* interfacial polycondensation between the functional amine monomers and trimesoyl chloride for arsenic removal from water and desalination of NaCl aqueous solution. The amine chemical structure is found to have a significant impact on the physicochemical properties, leading to the variation of permeation flux of the prepared membrane. The PA selective layer synthesized by aliphatic amine monomers has a more compact structure, which declines the permeation flux of the membrane. Despite providing the membrane with better thermal resistance, the aromatic amine monomers are observed to form a thicker, more rigid, and more hydrophobic selective layer, resulting in a low permeation flux. On the contrary, the PA layer produced by the cyclic PIP monomers with high hydrophilicity exhibits superior permeation flux and comparable As(v) and salt rejections. The derived membrane shows a reasonable permeation flux of 16.1 kg m<sup>-2</sup> h<sup>-1</sup> and *ca.* 99.9% rejection for 1.5 mg L<sup>-1</sup> As(v) removal, as well as 13 kg m<sup>-2</sup> h<sup>-1</sup> and 99.3% rejection for 30 g L<sup>-1</sup> NaCl separation at 60 °C. The good separation performance suggested the promising application of PA-TFC membrane for pervaporation removal of toxic arsenic from water and seawater desalination.

## Author contributions

Xuan Minh Pham: conceptualization, methodology, investigation, formal analysis. Thu Minh Le: methodology, investigation, formal analysis. Thien Trong Tran: investigation. Ha Phuong Ky Huynh: methodology, supervision. Mai Thanh Phong: conceptualization, methodology, supervision. Le-Hai Tran: conceptualization, methodology, formal analysis, supervision, writing – original draft. Van-Huy Nguyen: writing – review & editing, supervision.

## Conflicts of interest

The authors declare that they have no known competing for financial interests or personal relationships that could have influenced the work reported in this paper.

## Acknowledgements

This research is funded by the Ho Chi Minh City University of Technology, Viet Nam National University Ho Chi Minh City under grant number T-KTHH-2020-12. We acknowledge the support of time and facilities from Ho Chi Minh City University of Technology (HCMUT), VNU-HCM for this study.

## Notes and references

- 1 F. E. Ahmed, R. Hashaikeh and N. Hilal, Hybrid technologies: The future of energy efficient desalination—A review, *Desalination*, 2020, **495**, 114659.
- 2 I. Ihsanullah, M. A. Atieh, M. Sajid and M. K. Nazal, Desalination and environment: A critical analysis of impacts, mitigation strategies, and greener desalination technologies, *Sci. Total Environ.*, 2021, 146585.
- 3 J. M. Gohil and P. Ray, A review on semi-aromatic polyamide TFC membranes prepared by interfacial polymerization: Potential for water treatment and desalination, *Sep. Purif. Technol.*, 2017, **181**, 159–182.
- 4 Q. Wang, N. Li, B. Bolto, M. Hoang and Z. Xie, Desalination by pervaporation: A review, *Desalination*, 2016, **387**, 46–60.
- 5 W. Kaminski, J. Marszalek and E. Tomczak, Water desalination by pervaporation—Comparison of energy consumption, *Desalination*, 2018, **433**, 89–93.
- 6 I. Prihatiningtyas and B. Van der Bruggen, Nanocomposite pervaporation membrane for desalination, *Chem. Eng. Res. Des.*, 2020, **164**, 147–161.
- 7 R. Castro-Muñoz, Breakthroughs on tailoring pervaporation membranes for water desalination: A review, *Water Res.*, 2020, 116428.
- 8 S. G. Chaudhri, B. H. Rajai and P. S. Singh, Preparation of ultra-thin poly (vinyl alcohol) membranes supported on polysulfone hollow fiber and their application for production of pure water from seawater, *Desalination*, 2015, **367**, 272–284.
- 9 Y. K. Ong, G. M. Shi, N. L. Le, *et al.*, Recent membrane development for pervaporation processes, *Prog. Polym. Sci.*, 2016, **57**, 1–31.
- 10 M. B. M. Y. Ang, S.-H. Huang, S.-W. Wei, *et al.*, Surface Properties, Free Volume, and Performance for Thin-Film Composite Pervaporation Membranes Fabricated through Interfacial Polymerization Involving Different Organic Solvents, *Polymers*, 2020, **12**(10), 2326.
- 11 Q.-F. An, M. B. M. Y. Ang, Y.-H. Huang, *et al.*, Microstructural characterization and evaluation of pervaporation performance of thin-film composite membranes fabricated through interfacial polymerization on hydrolyzed polyacrylonitrile substrate, *J. Membr. Sci.*, 2019, **583**, 31–39.
- 12 S.-H. Huang, C.-J. Hsu, D.-J. Liaw, C.-C. Hu, K.-R. Lee and J.-Y. Lai, Effect of chemical structures of amines on physicochemical properties of active layers and dehydration of isopropanol through interfacially polymerized thin-film composite membranes, *J. Membr. Sci.*, 2008, **307**(1), 73–81.
- 13 S.-H. Huang, W.-S. Hung, D.-J. Liaw, *et al.*, Interfacially polymerized thin-film composite polyamide membranes: Effects of annealing processes on pervaporative dehydration of aqueous alcohol solutions, *Sep. Purif. Technol.*, 2010, **72**(1), 40–47.
- 14 C.-L. Li, S.-H. Huang, D.-J. Liaw, K.-R. Lee and J.-Y. Lai, Interfacial polymerized thin-film composite membranes for pervaporation separation of aqueous isopropanol solution, *Sep. Purif. Technol.*, 2008, **62**(3), 694–701.
- 15 Y. Li, Y. Su, Y. Dong, *et al.*, Separation performance of thin-film composite nanofiltration membrane through interfacial polymerization using different amine monomers, *Desalination*, 2014, **333**(1), 59–65.
- 16 H.-A. Tsai, T.-Y. Wang, S.-H. Huang, *et al.*, The preparation of polyamide/polyacrylonitrile thin film composite hollow fiber membranes for dehydration of ethanol mixtures, *Sep. Purif. Technol.*, 2017, **187**, 221–232.
- 17 S.-H. Huang, Y.-Y. Liu, Y.-H. Huang, *et al.*, Study on characterization and pervaporation performance of interfacially polymerized polyamide thin-film composite membranes for dehydrating tetrahydrofuran, *J. Membr. Sci.*, 2014, **470**, 411–420.
- 18 W. Cha-Umping, E. Hosseini, A. Razmjou, M. Zakertabrizi, A. H. Korayem and V. Chen, New molecular understanding of hydrated ion trapping mechanism during thermally-driven desalination by pervaporation using GO membrane, *J. Membr. Sci.*, 2020, **598**, 117687.
- 19 K. Guan, G. Liu, H. Matsuyama and W. Jin, Graphene-based membranes for pervaporation processes, *Chin. J. Chem. Eng.*, 2020, **28**(7), 1755–1766.
- 20 A. Huang and B. Feng, Synthesis of novel graphene oxide-polyimide hollow fiber membranes for seawater desalination, *J. Membr. Sci.*, 2018, **548**, 59–65.
- 21 X. Zhao, Z. Tong, X. Liu, J. Wang and B. Zhang, Facile Preparation of Polyamide–Graphene Oxide Composite Membranes for Upgrading Pervaporation Desalination Performances of Hypersaline Solutions, *Ind. Eng. Chem. Res.*, 2020, **59**(26), 12232–12238.
- 22 J. A. D. Marquez, M. B. M. Y. Ang, B. T. Doma Jr, *et al.*, Application of cosolvent-assisted interfacial polymerization technique to fabricate thin-film composite polyamide pervaporation membranes with PVDF hollow fiber as support, *J. Membr. Sci.*, 2018, **564**, 722–731.
- 23 C. Cheng, P. Li, T. Zhang, X. Wang and B. S. Hsiao, Enhanced pervaporation performance of polyamide membrane with synergistic effect of porous nanofibrous support and trace graphene oxide lamellae, *Chem. Eng. Sci.*, 2019, **196**, 265–276.
- 24 R. Mehta, H. Brahmabhatt, G. Bhojani and A. Bhattacharya, Polypyrrole as the interlayer for thin-film poly (piperazine-amide) composite membranes: Separation behavior of salts and pesticides, *J. Appl. Polym. Sci.*, 2021, **138**(18), 50356.
- 25 S.-H. Huang, W.-S. Hung, D.-J. Liaw, *et al.*, Positron annihilation study on thin-film composite pervaporation membranes: Correlation between polyamide fine structure

- and different interfacial polymerization conditions, *Polymer*, 2010, **51**(6), 1370–1376.
- 26 M. B. M. Y. Ang, V. Lau Jr, Y.-L. Ji, *et al.*, Correlating PSf support physicochemical properties with the formation of piperazine-based polyamide and evaluating the resultant nanofiltration membrane performance, *Polymers*, 2017, **9**(10), 505.
- 27 S.-T. Kao, S.-H. Huang, D.-J. Liaw, *et al.*, Interfacially polymerized thin-film composite polyamide membrane: positron annihilation spectroscopic study, characterization and pervaporation performance, *Polym. J.*, 2010, **42**(3), 242–248.
- 28 Y. Liu, Z. Tong, H. Zhu, X. Zhao, J. Du and B. Zhang, Polyamide composite membranes sandwiched with modified carbon nanotubes for high throughput pervaporation desalination of hypersaline solutions, *J. Membr. Sci.*, 2022, **641**, 119889.
- 29 B. Liang, W. Zhan, G. Qi, *et al.*, High performance graphene oxide/polyacrylonitrile composite pervaporation membranes for desalination applications. 10.1039/C4TA06573E, *J. Mater. Chem. A*, 2015, **3**(9), 5140–5147, DOI: 10.1039/C4TA06573E.
- 30 I. Prihatiningtyas, G. A. Gebreslase and B. Van der Bruggen, Incorporation of Al<sub>2</sub>O<sub>3</sub> into cellulose triacetate membranes to enhance the performance of pervaporation for desalination of hypersaline solutions, *Desalination*, 2020, **474**, 114198, DOI: 10.1016/j.desal.2019.114198.
- 31 Y. Qian, X. Zhang, C. Liu, C. Zhou and A. Huang, Tuning interlayer spacing of graphene oxide membranes with enhanced desalination performance, *Desalination*, 2019, **460**, 56–63, DOI: 10.1016/j.desal.2019.03.009.
- 32 Z. Xie, M. Hoang, T. Duong, D. Ng, B. Dao and S. Gray, Sol-gel derived poly(vinyl alcohol)/maleic acid/silica hybrid membrane for desalination by pervaporation, *J. Membr. Sci.*, 2011, **383**(1), 96–103, DOI: 10.1016/j.memsci.2011.08.036.
- 33 Y. L. Xue, J. Huang, C. H. Lau, B. Cao and P. Li, Tailoring the molecular structure of crosslinked polymers for pervaporation desalination, *Nat. Commun.*, 2020, **11**(1), 1461, DOI: 10.1038/s41467-020-15038-w.
- 34 G. Liu, J. Shen, Q. Liu, *et al.*, Ultrathin two-dimensional MXene membrane for pervaporation desalination, *J. Membr. Sci.*, 2018, **548**, 548–558, DOI: 10.1016/j.memsci.2017.11.065.
- 35 M. Drobek, C. Yacou, J. Motuzas, A. Julbe, L. Ding and J. C. Diniz da Costa, Long term pervaporation desalination of tubular MFI zeolite membranes, *J. Membr. Sci.*, 2012, **415–416**, 816–823, DOI: 10.1016/j.memsci.2012.05.074.
- 36 C. H. Cho, K. Y. Oh, S. K. Kim, J. G. Yeo and P. Sharma, Pervaporative seawater desalination using NaA zeolite membrane: Mechanisms of high water flux and high salt rejection, *J. Membr. Sci.*, 2011, **371**(1), 226–238, DOI: 10.1016/j.memsci.2011.01.049.
- 37 K. Cui, P. Li, R. Zhang and B. Cao, Preparation of pervaporation membranes by interfacial polymerization for acid wastewater purification, *Chem. Eng. Res. Des.*, 2020, **156**, 171–179, DOI: 10.1016/j.cherd.2020.01.022.